The object of this study is HSS API 5DP Gr 105 which has been used as drill pipe and was found leak during drilling activity, causing a delay in the delivery of drilling products. The interaction among the high partial pressure of H_2S, a high-hardness material, and the injection of high-density completion fluid (HDCF) remains poorly understood, leading to sulfide stress cracking. Despite offering substantial benefits, the detected trace amounts of hydrogen and sulfur indicate a localized corrosion, which can lead to unprecedented drilling shutdowns and consequently impose greater operational costs. Recently, the API 5DP 3-1/2" drill pipe experienced failure with a significant hardness value of 26 HRC, exceeding the standard specified by NACE MR 0175. The material was in service in rich H_2S gas well, where HDCF was injected to maintain hydrostatic pressure and serve as a control fluid. Multiple field and laboratory investigations have been undertaken to identify the root cause of this failure, including visual inspections, macrophotography, chemical composition analysis, completion fluid testing, tensile testing, metallography, and SEM-EDX analysis. The shear-slip and step-like markings on the failed material clearly indicate a brittle nature, correlating with a noticeable tensile strength of 907.80 MPa and an elongation limit of 18.18%. The increase in hardness beyond 22 HRC indicates susceptibility to sulfide stress cracking (SSC) where the hydrogen permeation increases with the increasing H2S partial pressure. These facts align with water chemistry analysis results to show S^{2-} and HS^{-} levels exceeding one ppm. Additionally, metallography reveals intergranular cracking in the tempered martensite, likely initiated at a local stress concentrator before propagating and confirmed by scanning electron microscope (SEM) images

Keywords: sulfide stress cracking, hydrogen embrittlement, sulfur content, drill pipe failure

UDC 622.24:620.178.3:620.19
DOI: 10.15587/1729-4061.2026.352272

UNVEILING THE ROOT CAUSE FAILURE 3-1/2" PARTED DRILL IN ONSHORE ENVIRONMENT

Sidhi Aribowo
PhD Student*
ORCID: https://orcid.org/0000-0002-7255-1931
Johny Soedarsono
Corresponding author
Doctor of Engineering, Professor
Prof Johny Wahyuadi Laboratory*
E-mail: jwsono@metal.ui.ac.id
ORCID: https://orcid.org/0000-0001-6051-2866
Sopar Simanullang
Assistant Manager Quality Control**
ORCID: https://orcid.org/0009-0005-6551-4816
Ario Oktora
Senior Supervisor QC 5th Area**
ORCID: https://orcid.org/0009-0002-0417-0042
Warneri
Manager Rig Operation V**
ORCID: https://orcid.org/0009-0005-8552-1634
Rini Riastuti
Doctor of Engineering, Senior Lecturer
Prof Johny Wahyuadi Laboratory*
ORCID: https://orcid.org/0000-0003-3431-0413
Agus Kaban
Doctor of Engineering
Prof Johny Wahyuadi Laboratory*
ORCID: https://orcid.org/0000-0002-9706-0506
*Department of Metallurgical and Materials Engineering
Universitas Indonesia
Kampus Baru UI Depok, Jawa Barat, Indonesia, 16424
**Pertamina Drilling Services Indonesia
MCC Building, Kuningan, Jakarta, Indonesia, 13140

Received 30.11.2025
Received in revised form 28.01.2026
Accepted 12.02.2026
Published 27.02.2026

How to Cite: *Aribowo, S., Soedarsono, J., Simanullang, S., Oktora, A., Warneri, W., Riasuti, R., Kaban, A. (2026). Unveiling the root cause failure 3-1/2" parted drill in onshore environment. Eastern-European Journal of Enterprise Technologies, 1 (1 (139)), 59–69. https://doi.org/10.15587/1729-4061.2026.352272*

1. Introduction

A systematic approach to attributing energy resources based on their carbon footprint is essential for the rapid advancement of oil and gas exploration through the drilling process. Their operational reliability depends on various factors, such as material properties, environmental conditions, and impurity components, which primarily serve to prevent failure when hydrocarbon fluids are transported through interconnected piping networks for the conveyance of single or multiple fluids [1]. Piping reliability is imperative, as failures often lead to higher operational costs. In this case, several flaws are often offset to disrupt the drilling activity such as H_2S gas impurities that induces the corrosion [2]. Additionally, the literature indicates that the presence of impurities such as H_2S or CO_2 significantly increases operational costs, amounting to nearly USD 1400 trillion annually [3]. This challenge emphasizes the importance of conducting failure and incident analyses, along with mitigation plans, to prevent future problems.

SSC emerges as a critical form of damage in high-strength steel materials when subjected to sour environments. Numerous issues related to drilling failures caused by SSC have

garnered significant attention from researchers and practitioners. Efforts to mitigate and prevent similar cases have been actively pursued. The paper [4] investigates the sulfide stress corrosion cracking (SSCC) of G105 and S135 pipe steel in a hydrogen sulfide (H_2S) environment using slow-strain-rate testing, ultimately concluding that the slow-strain-rate test reflects the pipe's susceptibility to SSCC. Furthermore, the study indicates that SSCC failure results from hydrogen diffusion, which diminishes the cohesive binding of iron atoms prior to fracture.

Previous work by [5] investigates the failure of S135 31/2″ drill pipe through the utilization of a scanning electron microscope and an energy dispersive spectrometer (EDS), including an examination of their physical and chemical properties. The comprehensive results suggest that the interaction between H_2S content and material susceptibility contributes to the rupture of the drill pipe. At the same time, the report of [6] shows the effort to improve the corrosion resistance of the same material by controlling the drill pipe tension. Moreover, the study offers a prediction to improve the SSC resistance by extending the material yield strength and tensile capacity at 125 ksi and nearly 20% of its original magnitude.

Indeed, the notion of attributing material failure exclusively to material susceptibility was not prominently featured in the depiction of the premature failure of high-strength steel (HSS) in sour environments. Moreover, this deficiency presents substantial barriers to entry and knowledge acquisition, thereby hindering the comprehension of HSS material failures under completion fluids and increased partial pressures of H_2S. Consequently, a comprehensive discourse on methodologies to identify the risks associated with sulfide stress cracking (SSC) and their mechanistic damage pathways-beyond the critical factors related to the trunnion that induce SSC – remains isolated, particularly when high density completion fluid (HDCF) is introduced into the sour well. Therefore, studies to unveil the root cause failure of the API 5DP material including the selected evaluation method is relevant.

2. Literary review and problem statement

The paper [7] presents the results of research of important insights into SSC mechanisms under wet H_2S exposures, particularly given that SSC has been a critical problem when high-strength carbon steel (HSCS) is used in deep wells. The same paper proposes modeling and investigating SSC in HSCS using C-110 material under various gas mixtures, including CH_4, CO_2, and H_2S at 280 ppm. The paper [8] elaborates on the SSC mechanism of the API X-100 through the implementation of a few tests, such as proof ring testing (NACE TM-0177) and electrochemical polarization techniques, before concluding that the corrosion pit becomes the primary source of crack initiation, where this site allows excessive hydrogen atom migration into the metal. However, the existing study remains difficult to qualify the effect of gas impurities on the susceptibility of the material against SSC.

But there were unresolved issues related to the partial pressure of CO_2 determines hydrogen permeation, and SSC resistance is considered the primary factor affecting SSC, the mechanism of SSC in the HSCS remains poorly understood. The paper [9] shows that controlling the pH level of the water determines the localized corrosion mechanism caused by dissolved CO_2 and H_2S gases, including the effect of temperature on minimizing chemical reaction acceleration and on gas solubility. Moreover, the research [10] shows that the presence of CO_2 in the annular space of flexible pipe decreases the fatigue resistance of HSCS. However, the study leaves a research gap that corresponds to the utilization of higher-grade corrosion-resistant alloy in the presence of environmental and corrosive species.

The reason for this may be corrosion-resistant alloys (CRAs) are compatible with addressing the impacts of high temperature, high pressure, and severe H_2S-corrosion environments. However, due to the performance-cost ratio, the mechanical properties of pertinent materials, such as HSCS, remain the key priority for drilling pipe. The paper [11] argued that gas fugacity, aqueous chemical activity, and ionic strength constitute several additional vital parameters that must be considered to challenge the material selection protocol before service. This consideration aims to mitigate the risk of environmentally-assisted cracking (EAC), such as SSC, in compliance with NACE MR0175/ISO 15156 standards for sour service. In addition, the same standard describes the indirect correlation between the strength of material and its resistance to SSC, with a maximum Rockwell hardness (HRC) of 22 [12]. A way to overcome these is to develop the idea to distill the EAC in API 5DP.

API 5DP G105 is often used as onshore drill pipe because of its balanced strength, toughness, and manufacturability, including production cost. The material undergoes quenching and tempering heat treatment during manufacturing to achieve high strength and the desired hardness, followed by a reheat treatment at a lower temperature to reduce brittleness and enhance toughness and ductility [13]. However, the material remains susceptible to experience hydrogen-assisted cracking, especially in a sour service environment without proper heat treatment and tempering process. Despite their yield strength offering a good balance between strength and reliability, higher load capacity, and reduced buckling risk to underpin onshore drilling, it is worth noting their hardness of 28–32 HRC and their corresponding vulnerability against SSC. For instance, the report [14] argues that the material remains susceptible to SSC under an H_2S-rich environment, especially when the exposure is unlimited. From herein after, API 5DP G105 is shortened to API 5DP.

While recent advancements have improved the assessment of HSS material susceptibility to SSC, a gap remains in comprehensive, field-based failure analysis studies. This approach was used and often-overlooked integration of factors such as controlling H_2S partial pressure, fractography, and service history in SSC failures results in speculative root-cause analyses and generic prevention methods. Consequently, it is crucial to investigate the H_2S source, which heightens the vulnerability of API 5DP materials to SSC, despite their compliance with API and NACE standards. Identifying the source of corrosive agent in the sour well is imperative for preventing sulfide stress cracking (SSC), as different generation mechanisms demand specific mitigation strategies. SSC results from hydrogen produced during H_2S-steel reactions. Still, the effectiveness of various chemicals, such as scavengers and biocides, and material choices depends on whether H_2S originates from formation fluids, bacteria, chemical decomposition, or well failures. Without proper identification of sources, mitigation efforts could be misused, hydrogen charging may continue, and the risk to SSC remains elevated even if standards are met.

All this gives reason to argue that it is expedient to conduct a study devoted to allow the comprehensive analysis in terms of failure of API 5DP material in high partial pressure of H_2S and addition of HDCF.

3. The aim and objectives of the study

The aim of this study is to delve into a more nuanced explanation of the primary effect of adding HDCF in the sour well on SSC in HSCS API 5DP Grade 105 material. This approach benefits practitioners and academia by improving their strategies to prevent initial material failure.

To achieve this aim, the following objectives were accomplished:

– verify the material grade and its compliance with standards, including its resistance to sour service, by utilizing inductively coupled plasma-optical emission spectroscopy (ICP-OES) of the exposed material and virgin material;

– assess the chemical compatibility of HDCF with the sour well conditions to prevent SSC, considering that the higher chloride content in HDCF may further accelerate corrosion;

– confirm the downhole load-bearing capacity of materials and their susceptibility to SSC, including measurements of resistance to deformation using tensile and hardness tests;

– examine the microstructure, cracks, and corrosion features of the failed material while identifying the actual elemental composition in the affected localized areas through metallography and SEM-EDS characterization.

4. Materials and methods

4. 1. The object and hypothesis of the study

The object of this study is HSS API 5DP Gr 105 which has been used as drill pipe and was found leak during drilling activity, causing a delay in the delivery of drilling products. The parted and cracked 3–1/2″ drill pipe material was used during well completion, where the recorded partial pressure of H_2S was at 0.6 psi. Based on the above argument, this work aims to identify and demonstrate the root cause of failure in the HSS API 5DP 105 ksi grade by testing the specimen material through mechanical and chemical methods. A case study of a drill pipe during well completion was included to investigate the primary material failure. It is suspected that sulfide stress cracking caused the failure, due to its hardness of 26 HRC and higher tensile tension, coupled with a high yield strength of 630 MPa, which makes it vulnerable to SSC and is assumed to occur according to NACE MR 0175.

Recent laboratory analyses of wellhead samples identified sulfide ions. This simplification research also systematically investigated alterations in microstructure and in the chemical and mechanical properties of the tube steels. A variety of assessments, including completion-fluid tests, chemical-composition analysis, tensile testing, hardness measurements, metallography, and SEM-EDS, were performed to determine the stress-corrosion cracking (SCC) fracture mode and its damage progression. The benefits of the selected methodologies are appraised through a comprehensive evaluation.

4. 2. Materials

API 5DP G 105 was used to assess the influence of hydrogen-induced cracking on the material and to understand the actual damage mechanism of an exposed drill pipe in a sour well. In this work, the selected material was a proprietary API 5DP Grade 105 pipe, and the steel's chemical composition (wt.%) was determined by inductively coupled plasma-optical emission spectroscopy (ICP, Perkin 7300DV). The as-received material from the bottom whole was prepared and analyzed as illustrated by Fig. 1.

Fig. 1. The as-received failed material of API 5DP Grade 105 R2

It is critical to note that the identity of the material is classified as API 5DP Grade 105 R2, where the steel grade 105 implies its yield strength of 105 ksi, material class of high-strength low-alloy steel and undergoes quenching and tempering. Furthermore, the dimensional identification of the failed and virgin material is critical before they undergone visual inspection (Fig. 2).

Fig. 2 shows the calculated length was 9.45 meters, the outer diameter (OD) was 88.9 mm, and the wall thickness was 9.35 mm. Recently, the material was selected and used as a drilling logger by a reputable oil and gas company, which reported the failure at a depth of 2743 mMD. In this case, HDCF with a specific gravity of 1.63 SG was introduced into the active well to replace the drill mud. The complete acronym of the manuscript is given in Table 1.

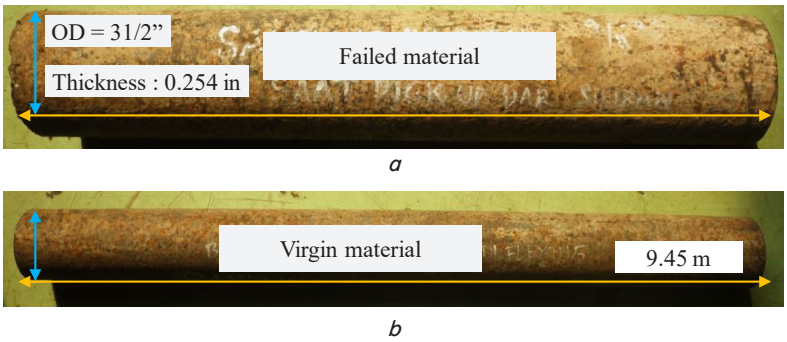

Fig. 2. The specimen: *a* — as-received fractured damage pipe exposed to chemicals; *b* — virgin pipe (non-exposed to chemicals)

Table 1

The paper acronym

Acronym	Remarks
mMD	Measured depth (datum)
Bbl	Barrel
TCB	Tubing casing brace
BHA	Bottom-hole assembly
HDCF	High-density completion fluid
Hi-vis	High visibility
SG	Specific gravity
DP	Drill pipe

The material has been utilized in the sour well completion stage, where the string is subjected to several stresses, such as

axial, bending, pressure, thermal, and residual stress, during manufacture. Moreover, the sourness of the well was captured by measuring the partial pressure of H_2S at 0.06 psia, based on the average monthly monitoring H_2S sample, at both the wellhead and flowline locations. The transfer of HDCF was executed alongside 40 bbl of Hi-Vis and 700 bbl of water after the TCB 6″ + BHA rotary assembly entered the well. The report indicates a failure in the drill pipe at joint 13 within the drill string (Fig. 2).

Leakage from DP 32 prompted the retrieval of the BHA, which was then brought to the surface. Upon inspection, a crack was identified on the crossover 3-7/8″ CAS PIN X 3-1/2″ IF BOX. In this case, CAS, PIN, X, 3-1/2″ IF Box, referring to the pipe having a casing-type connection, male thread, connected to a 3 1/2-inch internal flush (IF) female thread. The internal flush is a common standard API rotary shoulder in drill pipe and BHA components.

In this work, the evaluation of the fracture-damaged drill pipe was conducted in a structured manner. First, a visual analysis was performed to obtain a macroscopic understanding of the failure by collecting the sample from the site before assessing the condition of both the inner and outer sections of the drill pipe. Secondly, in cases of internal failure at the microscopic level of the pipe's interior, metallography and SEM-EDX analyses were performed by examining several points near the damaged area. In this context, the metallography test separates macro from micro examination. Lastly, mechanical property tests such as tensile and hardness tests complement the overall failure evaluation and investigation.

Based on the actual damage to the drill pipe, it is suspected that the material exposed to the HDCF experiences a more severe corrosion attack than that of virgin drill pipe (Fig. 2, *b*) that complies with mechanical, pressure, thermal, and environmental stresses during well completion. Accordingly, the emergence of a remarkable H_2S partial pressure and the continuous injection of HDCF-containing brine aggravate and accelerate the corrosion process.

4. 3. Completion fluid analysis

The water analysis was essential for examining water chemistry in detail, including total dissolved solids (TDS), resistivity, cations, and anions, which remained in the high-density completion fluid. In this study, 50 mL of water from the HDCF was sampled at two sites: the original completion fluid and the used well fluid. A sanitized polyethene bottle was used to collect samples, which were then stored at ambient temperature for further testing. Multiple ions were thoroughly analyzed to understand the failure mechanism of API 5DP material when exposed to HDCF completion fluid.

4. 4. Tensile and hardness test

It is crucial to measure and distinguish the stress level and ductility reduction in the failed material from those in the non-failed material before concluding the crack propagation pattern. In this case, only two tensile coupons were designed in accordance with ASTM E8 [15]. Tensile test specimens with a 5 mm diameter circular cross-section and a 30 cm gauge length were measured using the Instron 5982 testing machine at a displacement speed of 3 mm/min and 25°C. It is important to note that the surface of the tensile test specimen was polished with 400-grit SiC emery paper before testing. The specimen was then loaded to a tensile strain of 0.7% offset strain to evaluate the API 5DP material's susceptibility to SSC. These measurements were taken before determining the tensile strength, yield strength, and elongation of both the failed and virgin specimens.

For the hardness test, the cylindrical sample was prepared and machined at a specific longitudinal location at a strain rate of 1×10^{-3} s^{-1}. Meanwhile, the hardness test is a crucial parameter for assessing material failure, especially in identifying the metallurgical conditions that facilitate hydrogen cracking and the location of the hardness test was displayed in Fig. 3.

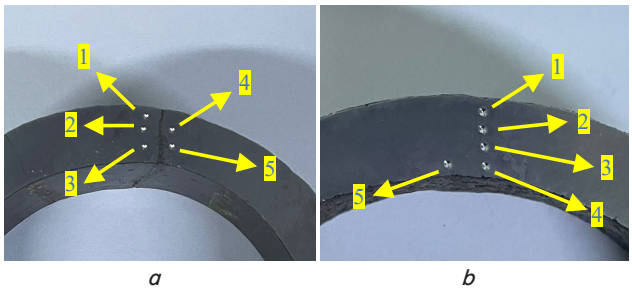

a *b*

Fig. 3. The location of indentation on the test specimen: *a* — as-received fractured damage pipe exposed to chemical; 1 — crack tip; 2, 3 — crack propagation west side; 4 — crack propagation east side; 5 — crack termination; *b* — virgin pipe (non-exposed to chemical); 1 — crack tip 2, 3 — crack propagation east side; 4 — crack termination east side; 5 — crack termination west side

In this study, the Rockwell hardness C test was performed on cross-sectional specimens from both failed and non-failed materials, in accordance with ASTM E18 standards, as illustrated in Fig. 3. In this case, the selected load was 10 kg and converted to the Rockwell hardness C scale (HRC). The number of indentations was made and selected in five locations in the proximity of the test specimen to evaluate their susceptibility to cracking.

4. 5. Metallography examination

Characterizing the microstructure is directly linked to the susceptibility features of SSC, emphasizing the microstructural differences between failed and non-failed materials. Two specimens were provided for macrostructural observation before their microstructure was further examined under an optical microscope. The test specimen was taken from both the failed and virgin material of API 5DP Grade 105, as illustrated in Fig. 4.

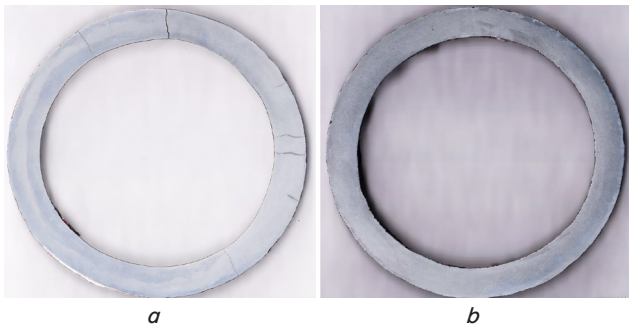

a *b*

Fig. 4. The macrostructure of the test specimen for examination: *a* — failed specimen; *b* — virgin specimen

A specimen section was taken near the fracture origin, mounted in phenolic resin, ground with 240-grit SiC paper, and polished with a 1 μm alumina suspension before they are available to test as appeared in Fig. 4. To reveal the microstructure

components, a 3% Nital solution was applied to the surface, and observations were performed using an Olympus GX51 microscope with magnifications ranging from 100x to 1000x.

4. 6. Surface morphology characterization

In this study, SEM-EDX analysis is conducted to elucidate the brittle and fracture morphologies, as well as the elemental composition, of both failed and non-failed materials, using a JEOL JSTM-IT500 equipped with X-ray spectroscopy relevant to SSC. Fig. 5 illustrates the prepared specimen used for SEM-EDS analysis. Based on a visual inspection, brittle cracks and ductile failure possibly present in the as-received tempered martensite API 5DP material led to cutting away samples from locations A and B. This was done to identify if the failure was caused by hydrogen-assisted cracking from the overloading drilling process or by environmental-assisted damage.

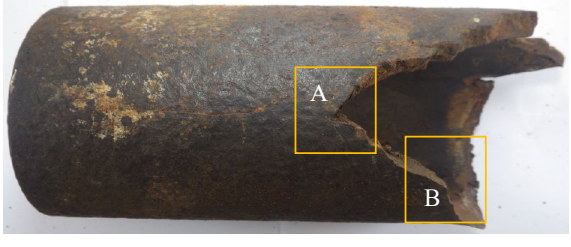

Fig. 5. The SEM-EDX location on the failed material: *a* — brittle crack; *b* — ductile failure

The specimen preparation process was quite extensive. The specimen was prepared by achieving a 1 × 1 cm coupon from areas A and B. Upon receipt, the specimens were cleaned ultrasonically in ethanol for 15 minutes to remove corrosion products and loose debris. An accelerating voltage of 20 kV was employed under high-vacuum conditions. Meanwhile, the scanning rate and step size for the failed material were 200 × 200 μm and 0.5 μm.

5. Results of API 5DP Gr 105 failure

5. 1. Chemical composition test

Table 1 shows the analyzed chemical composition of the tested API 5DP material, taken from the failed samples. Further, the chemical composition properties of the as-received drill pipe conform to the material specification of API 5D standard specification for Drill Pipe (Table 2).

Based on Table 2, the levels of phosphorus and sulfur are within acceptable limits [15]. It is also clear that the material composition meets the chemical requirements specified in NACE MR 0175 and is suitable for use in H_2S environments, although additional mechanical and hardness testing will be needed to confirm the results.

Therefore, material non-conformance is not considered a factor contributing to the failure.

It is also critical to note the carbon equivalent (CE) of the material, which corresponds to the material's hardenability and its effect on the risk of SSC. Equation 1 shows the calculation of the CE of the material [16]

$$CE = C + \frac{Si}{30} + \frac{Mn}{20} + \frac{Cu}{20} + \frac{Ni}{60} + \frac{Cr}{20} + \frac{Mo}{30} + \frac{V}{10} + 5B. \quad (1)$$

Based on the calculation, the CE for the failed material was 0.383, indicating high hardenability that allows hydrogen diffusion to create local hardening. An excess source of hydrogen indicates a higher concentration of hydrogen atoms that will diffuse into the material from the high partial pressure of H_2S.

5. 2. The completion fluid analysis result

The main goal of the completion fluid analysis is to evaluate the fluid chemistry before and after the HDCF injection into the sour well to maintain formation pressure and prevent formation fluid influx. In this case, the virgin completion fluid corresponds to the completion fluid before the addition of HDCF, and the used completion fluid is attributed to the completion fluid after the addition of HDCF. Thus, it is imperative to collect data on the chemical composition and its corresponding ions. Table 3 presents the water-chemistry results for the original completion fluid (before injection) and the used completion fluid (after injection).

Based on Table 3, the concentration of chloride ions at 517.15 ppm is considerably high, as it is the primary content of the high-density completion fluid. In this instance, components of HDCF, such as $CaCl_2$ and NaCl, are intentionally added to increase the fluid's density. It is critical to note that when the HDCF was injected into the well, it mixed with the drilling fluid and formation water, thereby increasing the dominance of chloride in the well.

Table 3

Completion fluid analysis result

Test	Methods	Unit	Result	
			Virgin	Used
TDS	Gravimetric	g/L	58.21	57.18
pH	pH meter	–	10.43	9.82
Sodium (Na^+)	Inductive coupled plasma	mg/L	–	17189.4
Calcium (Ca^{2+})	Inductive coupled plasma	mg/L	–	< 0.10
Barium (Ba^{2+})	Inductive coupled plasma	mg/L	–	64.8
Magnesium (Mg^{2+})	Inductive coupled plasma	mg/L	–	< 0.10
Bromide (Br^-)	Ion chromatography	ppm	14.3	12.5
Chloride (Cl^-)	Ion chromatography	ppm	273.15	517.15
Bisulfide (HS^-)	Titrimetric	ppm	–	< 1
Sulfide (S^{2-})	Spectrophotometer	ppm	–	340

Table 2

Chemical composition test results

Code	C (%)	Mn (%)	P (%)	S (%)	Si (%)	Ni (%)	Cr (%)	Mo (%)	Cu (%)
Specimen	0.25	1.25	0.007	0.005	0.25	0.013	0.86	0.28	0.015
API 5DP G105	–	–	0.03 (Max)	0.03 (Max)	–	–	–	–	–

According to laboratory analysis, the pH values of the virgin and used HDCF decreased from 10.43 to 9.82, equivalent to a 5.8% decrease. Laboratory analysis of the used HDCF detected bisul-

fide (HS^-) and sulfide (S^{2-}), indicating trace amounts of hydrogen sulfide (H_2S), along with the increasing chloride content of the well, which may accelerate pitting corrosion. It is also clear that the HDCF solution contains several addition cations such as Ba^{2+}, Ca^{2+}, Na^+, and Mg^{2+}.

5. 3. Tensile and hardness test results

Table 4 presents the tensile test results for both non-failed and failed materials after exposure to HDCF, evaluating changes in the manufacturing process and their variation during drilling operations to ascertain the cause of the drill pipe failure.

The tensile testing and yield strength results of the failed material are marginally lower than those of the pristine drill sample (Table 4). The tensile and yield strengths of the failed material are 907.90 MPa and 831.03 MPa, respectively. In contrast, the virgin drill pipe exhibits higher values of 909.67 MPa and 849.70 MPa. These observations suggest that the sole mechanical properties are unlikely to be the primary cause of the material's failure. Instead, the evidence points to environment-assisted failure as the more prevalent factor contributing to the increased fragility of API 5DP, which, in turn, creates a more aggressive chloride environment that deteriorates the exposed material.

Table 5 displays the resultant of the hardness test, intended to analyze the variations in hardness and their correlation with the tendency of SSC due to embrittlement and cracking.

Table 4

Tensile properties of the drill pipe

Specimen	Tensile strength (MPa)	Yield strength (MPa)	Elongation (%)
Failed drill pipe	907.80	831.03	18.18
Virgin drill pipe	909.67	849.70	18.47
API 5DP G 105	Min 793	724–931	Min. 12.5

Table 5

Hardness test of the drill pipe

Specimen	Rockwell C hardness (HRC)					
	Point of indenter					
	1	2	3	4	5	Average
Failed drill pipe	24.4	26.6	26.8	26.4	27.3	26.3
Virgin drill pipe	26.0	26.1	27.6	26.4	26.3	26.5

According to Table 5, the material's hardness in the failed specimen indicates its susceptibility to SSC. Except for the tensile test value, hardness or strength is often cited as a critical factor affecting the SSC resistance of API 5DP material.

Based on NACE MR 0175 or ISO 15156-1, the maximum hardness value of carbon steel in the sour service H_2S-containing well should be less than HRC 22. The variation in hardness value between the failed material and the virgin drill pipe indicates the material is susceptible to SSC. The failed drill pipe has a comparable low hardness of 26.3 HRC than that of virgin drill pipe, due to over-tempering from frictional heating and downhole temperature, as indicated by martensite softening [17].

5. 4. Surface morphology results

Fig. 6 shows the metallography characterization to reveal the failed and virgin material to elucidate the material's susceptibility to SSC. In this case, the macrostructure of the virgin material shows no cracks detrimental to SSC resistance and no discontinuities (Fig. 3). In consonance, the macrostructural evaluation is acceptable for SSC service and meet acceptance requirements of NACE MR 0175/ISO 15156. On the contrary, the macrostructural examination for the failed material reveals a crack, where the presence of the macrostructural cracks renders the material rejection for SSC service as per the same standard.

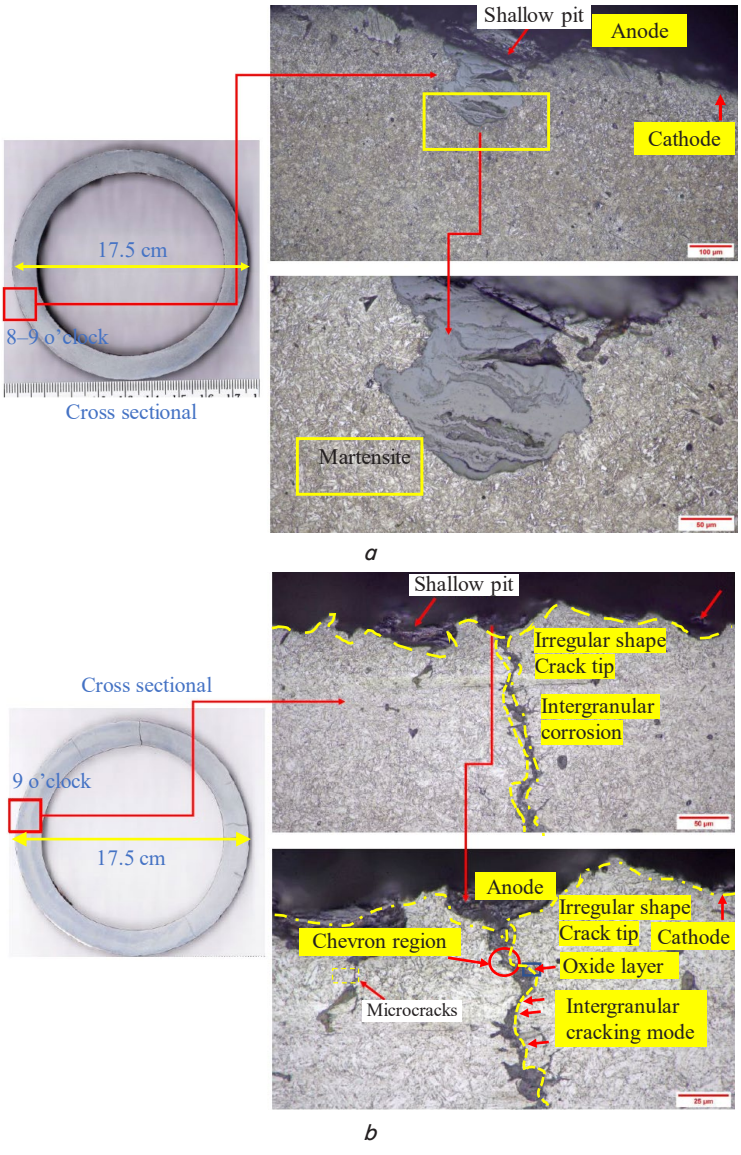

Fig. 6. The metallography result of API 5DP Grade 105: *a* – virgin material; *b* – the failed material

The photograph was taken from a cross-sectional view, capturing the microstructure from the 8–9 o'clock position, with the specimen measuring 17.5 cm in diameter (Fig. 6, *a*). It is noteworthy to note that the region near the shallow pit was magnified as shown in the lower photograph. Shallow pits are visible on the outer surface of the test specimen, although these are not necessarily benign corrosion features. It is suspected that these sites could be sites where hydrogen

atoms accumulate, potentially leading to crack initiation when exposed to sour conditions with HDCF injection. The material was heat-treated through quenching and tempering, resulting in tempered martensite, as shown in Fig. 6, *a*. The surface appears free of microcracks, indicating no exposure to HDCF. Additionally, the material demonstrates ductility, with a ductility value exceeding that of the API 5DP Gr 105 standard material, at 18.47% compared to 12.5%. (Table 4).

In contrast, the failed material shows evidence of SSC, as seen in the macro view of the ring specimen with observable circumferential cracking. Additionally, metallographic evidence indicates that shallow surface pits act as initiation sites for cracks, with subsurface microcracks emanating from lower pits and coalescing into a main crack that propagates perpendicular to the surface, with minimal associated plastic deformation [18]. Notably, the crack restricts plastic deformation, and its direction is necessarily perpendicular to the surface before the elongation decreases to 18.18% relative to the virgin material. Additionally, the trace of intergranular cracking mode is evident. The presence of chevron marks is conspicuous on the fractured material, indicating the direction of crack propagation and signifying the application of sustained tensile stress [19]. This information is essential to shed light on the SSC behavior of API 5DP material, which shows a few microcracks.

Fig. 7 shows full images of the fracture surfaces from the failed material, taken from two regions to better illustrate the material's brittle and ductile nature.

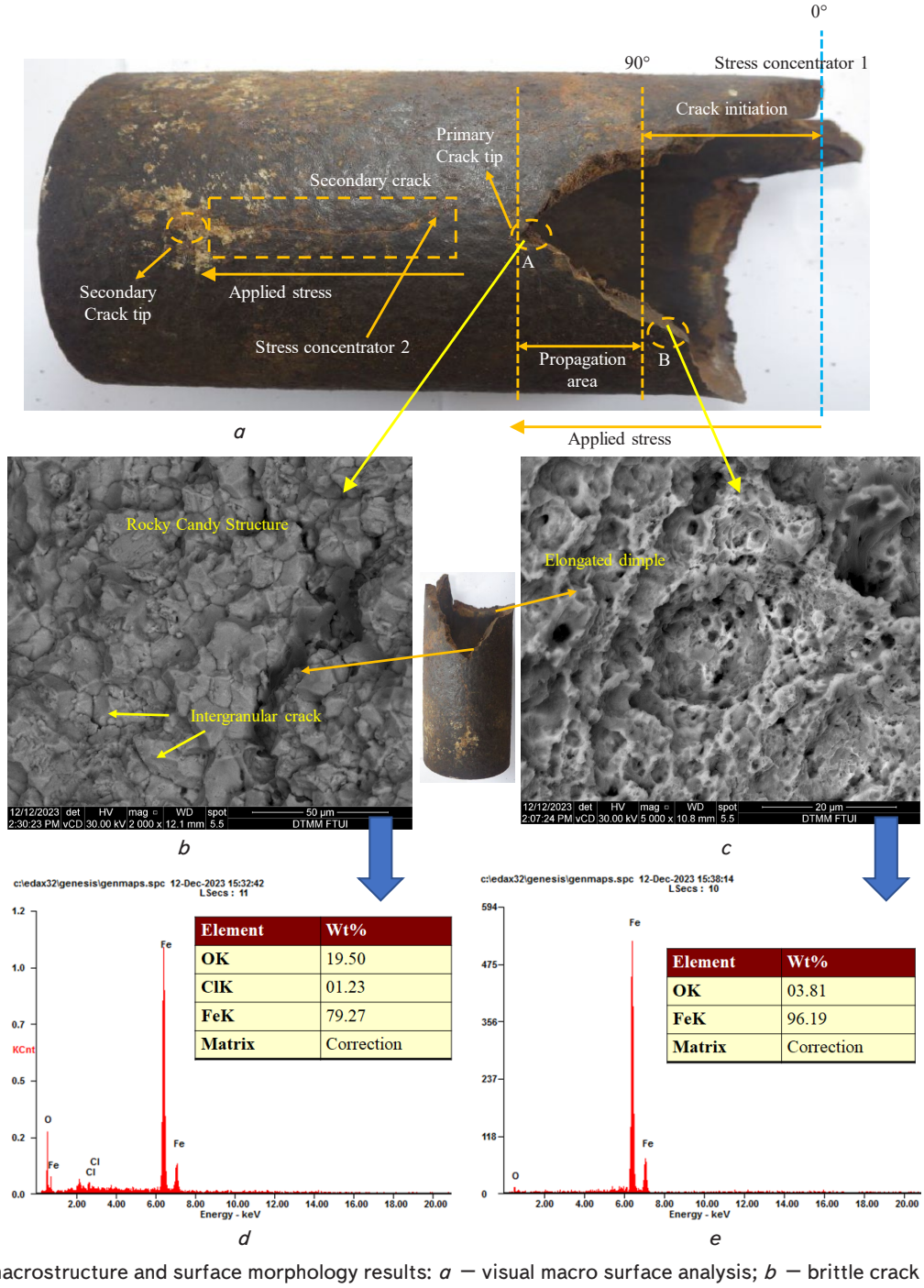

Fig. 7. The macrostructure and surface morphology results: *a* — visual macro surface analysis; *b* — brittle crack propagation; *c* — ductile failure (shear slip); *d* — elemental of brittle crack; *e* — elemental of ductile failure

Based on Fig. 7, *a*, there are at least two prominent stress concentrations at the shear slip edge and the center of the failed specimen. The ascertainment scenario is illustrated as follow; the stress concentrator acts as an initiation crack, starting early and propagating before reaching the pipe's center, where the angle shifts from 0° to 90°. It is worthy to note that the presence of HDCF intensifies the SSC mechanism especially in the presence of H_2S and high tensile stress. The region of crack initiation is significantly larger than the area of crack propagation before ceasing at the primary crack tip. Additionally, a secondary stress concentrator becomes evident, featuring a blunt edge that reduces tensile stress amplification, thereby promoting local hydrogen-assisted crack initiation.

The appearance of a brittle crack at location A indicates the presence of SSC, marked by plastic deformation at the crack tip (Fig. 7, *b*). This condition is strongly linked to a slightly lower yield strength of the failed material, measured at 831.03 MPa, compared to the original material. Although this value exceeds the yield strength of API 5DP standard material, it still increases SSC vulnerability. Additionally, the brittle crack is associated with a high elongation percentage, which allows SSC crack propagation to occur more readily (18.8% versus 12.5%). The SEM result confirms the metallography result, as the presence of intergranular cracks is evident in the brittle crack location. This result is comparable to the research result [20]. In the event of ductile failure at location B, the failed material demonstrates good plastic deformation capability, and the higher hardness correlates with the significant section loss and the presence of elongated dimples (Fig. 7, *c*). Apart from corrosion products of Fe and oxygen (O), EDX analysis indicates that the brittle fracture results from exposure to a chloride-rich sour environment, with 1.23 wt.% chloride present. In contrast, ductile failure is primarily influenced by Fe (96.19 wt.%) and O (3.81 wt.%), leaving little opportunity for aggressive chloride ions to participate in the fracture process.

6. Discussion on the failure of the material

Table 1 shows a similar chemical composition of the pipe body material, all of which meet the requirements for API 5DP Gr 105 in service according to NACE MR 0175. Emphasis is placed on low Nickel (Ni) content at 0.013 wt.% to demonstrate that the material is more vulnerable to SCC than other low-alloy steel of comparable hardness level [21]. Except for Ni, the Sulfur and Phosphorus content remain non-contributing factors in the failure, as the formation of bulk sulfur in steel may occur as MnS inclusions, while SSC is governed by environmental sulfur. In addition, the presence of Phosphorous is not accountable for controlling hydrogen uptake, which is closely related to the SSC mechanism [22]. However, it is noteworthy that the specimen's Mo content is relatively low at 0.28 wt.%, compared to the critical value of 0.75 wt.% required to improve strength and achieve SSC resistance in API 5DP material [23]. This identification point is essential for establishing the root cause of the material's failure (1). Additionally, the prominent CE from Equation (1) indicates higher hardenability and an increased risk of yielding hard martensite.

The chemistry evaluation includes several noticeable ions that may be present in the sour well fluid. The HDCF is considered a contributor to increased aggressive, corrosive ionic species in the well, such as Cl^- and Br^- (Table 3). The presence of HDCF is independent of the damage mechanism of API 5DP material due to SSC. On contrary, the SSC is dependent on the types of cations present in the HDCF injected solution. It is acceptable that corrosive nature can be rated in order of aggressiveness from most to least as follows: Ca^{2+}, Mg^{2+}, Na^+, and K^+. In this case, the rise in corrosion aggressiveness is caused by higher charge density and the strong corrosion-promoting effect, which is easily hydrolyzed [24]. These ions can serve as precursors, increasing H_2S solubility and SSC corrosion risk.

Similarly, the HDCF itself exhibits free oxygen and pH control, despite the chemical injected into the H_2S well promoting lower pH and allowing H_2S to dissolve. This fact aligns with the decrease in pH from 10.4 to 9.82 (Table 3). It is important to note that high partial pressure results from both a high H_2S mole fraction and a high system pressure. In this sense, under high system pressure, H_2S is released from solution, thereby elevating the effective H_2S partial pressure at the API 5DP material surface. The injected chemical creates sour conditions when it interacts with API 5DP material, thereby entrapping dissolved H_2S and confirming the observation of detectable bisulfide at less than 1 ppm and sulfide ions at 340 ppm in the post-injection completion fluid (Table 3).

The mechanical properties results indicate that tensile strength (TS) and yield strength (YS) are partially essential parameters to indicate the failure of API 5DP material. Based on Table 4, the TS and YS values for virgin and failed material are consistent, confirming that the material itself is susceptible to SSC. The higher TS value corresponds to higher hardness, which provides more space for hydrogen embrittlement. Typically, the SSC failure rises sharply beyond 754 MPa, and thus the two materials are subjected to SSC based on the TS values of 907.80 MPa and 909.67 MPa (Table 4). This increased tensile strength enables the pit formation initiator in API 5DP material, resulting from combined hydrogen build-up and reduced fracture toughness. The potential role for hydrogen in a hydrogen-rich environment, where hydrogen accumulation reduces the interfacial binding energy of iron, thereby promoting dislocation movement [25]. Furthermore, the elongation similarity between the two specimens is exempted from the SSC resistance requirement, even though the specimens' yield strengths exceed the standard elongation of API 5D material. In fact, the hardness values for both materials were confirmed to exceed the critical hardness value specified in NACE MR 0175. The high hardness is consistent with the metal's preparation during the manufacturing stage. However, increases magnitude of tensile stress is closely related to the hardness of material.

Aside from tensile strength, hardness and microstructure are frequently considered key factors influencing SSC resistance in steel. The indirect relationship between hardness and SSC resistance has led international standards to prioritize limiting steel hardness in H_2S environments [26]. In this work, the calculated value of hardness both for virgin and failed material is approximately 26 HRC to indicate a strong interplay between the hydrogen atoms and integranular crack that mainly dominate the hardness of steels. It is critical to compare the hardness of material API 5DP Gr 105 with the same grade such as API 5DP S135 in terms of their susceptibility against SSC. Theoretically, the rise of HRC correlated to the hydrogen permeation to the steel before they demonstrate the brittle fracture and crack of SSC [27].

The presence of an iron oxide layer and the non-SSC corrosion process indicate general corrosion, and the trace of tempered martensite is evident. Likewise, when drill pipe material is exposed to a well, the combination of high tensile strength, the presence of corrosive H_2S, and free water establishes the formation of anodic and cathodic sites. In this case, the anodic site is marked in the black area where the dissolution of metal

occurs. Meanwhile, the cathodic site is highlighted at the crack flanks behind the crack tip and on the surrounding external surface (lower stress level). The formation of a micro-galvanic cell is obvious, including the anodic movement, which is critical in the longitudinal direction [28]. The high hardness value of 26.3 HRC vs 22 HRC (NACE MR 0175) signifies the hydrogen absorption and detection of anodic site and favorable condition for SSC (Fig. 6, *a*, *b*), including the presence of intergranular (IG) cracking and corrosion.

The appearance of chevron marks to indicate the direction of crack propagation and signifies the brittle fracture nature of the failed material. As the stress increases under corrosive environment, the crack propagates in brittle fashion shown in chevron marks. Also, the chevron marks elicit the transition from slow SSC to fast final fracture along the grain boundary until it reaches the crack tip where the stress dominates and establish during unstable crack propagation.

It is important to note that the results for tensile, hardness, and microstructure align with the SSC. In this context, the clear linear relationship between H_2S partial pressure- exceeding 0,004 psia- and both tensile strength and hardness (greater than 620 MPa and 22 HRC) rules out the need to consider other types of wet H_2S damage, such as hydrogen-induced cracking (HIC), stress-oriented hydrogen-induced cracking (SOHIC), and blistering. Supporting this, SOHIC can be mitigated through post-weld heat treatment (PWHT), while HIC usually results from reduced residual stress.

Fig. 7 illustrates the mechanistic crack in the failed material, highlighting two potential stress concentrator points. The initial stress concentration occurs at the crack tip before it propagates leftward, causing the crack angle to increase from 0° to 90° (Fig. 7, *a*). Later, a secondary stress concentration appears at the center of the specimen before it extends in the same direction under the applied stress. The brittle nature at the primary crack tip is evident, with a rocky-candy structure and intergranular cracking confirming results from the metallography test (Fig. 7 *b*) [29]. Simultaneously, a few elements such as chloride at 1.23 wt.% and oxygen at 19.50 wt.% serve as strong indicators of HDCF dissolution in the failed material, as shown in Fig. 7, *d* in the A region. Additionally, Fig. 7, *c* clearly displays a porous structure with elongated dimples in the B region. The high content of Fe (96.19 wt.%) and O (3.81 wt.%) suggests that the material prolongs the transition from elastic to plastic deformation where the most possible general corrosion occur [30].

The limitations of this study are related to identifying the underlying cause of failure attributed to SSC, despite the presence of minor causes such as hydrogen embrittlement. However, hydrogen embrittlement can be excluded based on laboratory analysis reports indicating high concentrations of hydrogen bisulfide and sulfide ions. Furthermore, the shortcomings of this study correspond with the types of laboratory characterizations performed, including ring tests and bend tests. It is recommended to conduct these tests to determine the stress intensity factor threshold and to acquire strain values of failed and in-service materials, following NACE TM 0177 standards. Moving forward, the current testing methods are inadequate for preventing SSC through design modifications; therefore, controlling material hardness, microstructure, environment, and applied stress is essential to mitigate SSC. Additionally, development of techniques such as controlling heat treatment processes to achieve tempered bainite or ferrite-pearlite structures may be required. Post-weld heat treatment (PWHT) is also considered effective in controlling material hardness to less than 22 HRC.

Additionally, a strategy should be in place to prevent the initial failure of the material. Several approaches can be proposed and implemented, such as limiting H_2S with H_2S scavenger injection to reduce the presence of HS^- and S^{2-} ions and to control the overall H_2S partial pressure in the gas phase. Since the welding activity involves significant chloride ions, applying a corrosion inhibitor could be effective. This chemical also helps reduce hydrogen production by controlling electrochemical reactions when API 5DP pipe is exposed to corrosive environments containing H_2S, CO_2, and chloride in gas and water phases. This strategy is aligned with the result of low pH of the well fluid based on the laboratory outcome. Accordingly, the dosage of HDCF should also be pondered despite their effectiveness in commencing the drilling process. Upgrading the material, like choosing low-strength carbon steel compliant with NACE MR 0175, can also be advantageous. Furthermore, consistent inspection and monitoring such as measuring H_2S concentration, pH, and water content are essential to ensure the drill pipe's reliability.

7. Conclusions

1. The material grade of failed and virgin material complies the API 5DP standard in the sour service based on the chemical composition data. The presence of Phosphorous, Sulfur, Molybdenum, are significant to demonstrate the material in-service under H_2S environment.

2. Based on the chemistries of the liquid taken from the well, the presence of chloride, bisulfide, and hydrogen sulfide is clear to show that the high concentration of H2S and aggressive ions participate to accelerate corrosion process. However, it is noteworthy to note that the HDCF itself has a partial impact on the corrosion process.

3. The high TS and YS show the response of API 5DP material towards the stress at the crack tip accommodation. High value of TS causes the limitation for the plastic relaxation stress of material when subjected to drilling activity and amplify local stress while enhancing hydrogen damage.

4. The result of microstructure evaluation shows the presence of martensite microstructure. The anodic site is located in the dark area where the crack tip initiates before they propagate as more hydrogen uptake enter the metal. The intergranular corrosion and cracking are given to signify the corrosion and cracking process.

Conflict of interest

The authors declare that they have no conflict of interest in relation to this study, whether financial, personal, authorship or otherwise, that could affect the study and its results presented in this paper.

Financing

The study was performed without financial support.

Data availability

Data cannot be made available for reasons disclosed in the data availability statement.

Use of artificial intelligence

The authors confirm that they did not use artificial intelligence technologies in creating the submitted work.

Authors' contributions

Sidhi Aribowo: Writing – original draft, Visualization, Data curation, Resources, Investigation; **Johny Wahyuadi Soedarsono**: Validation, Methodology, Conceptualization, Supervision; **Sopar Mangarapot Simanullang**: Resources, Investigation, Data Curation; **Ario Oktora**: Resources, Investigation, Data Curation; **Warneri**: Resources, Investigation, Data Curation, Supervision, Project administration; **Rini Riastuti**: Validation, Methodology, Conceptualization, Supervision; **Agus Paul Setiawan Kaban**: Writing – review & editing, Supervision, Investigation, Validation.

References

1. Manzano-Ruiz, J. J., Carballo, J. G. (2024). Multiphase Transport of Hydrocarbons in Pipes. John Wiley & Sons. https://doi.org/10.1002/9781119888543
2. Kaban, A. P. S., Soedarsono, J. W., Mayangsari, W., Anwar, M. S., Maksum, A., Ridhova, A., Riastuti, R. (2023). Insight on Corrosion Prevention of C1018 in 1.0 M Hydrochloric Acid Using Liquid Smoke of Rice Husk Ash: Electrochemical, Surface Analysis, and Deep Learning Studies. Coatings, 13 (1), 136. https://doi.org/10.3390/coatings13010136
3. Tamalmani, K., Husin, H. (2020). Review on Corrosion Inhibitors for Oil and Gas Corrosion Issues. Applied Sciences, 10 (10), 3389. https://doi.org/10.3390/app10103389
4. Luo, S., Liu, M., Shen, Y., Lin, X. (2019). Sulfide Stress Corrosion Cracking Behavior of G105 and S135 High-Strength Drill Pipe Steels in H_2S Environment. Journal of Materials Engineering and Performance, 28 (3), 1707–1718. https://doi.org/10.1007/s11665-019-03913-7
5. Han, Y., Zhao, X., Bai, Z., Yin, C. (2014). Failure Analysis on Fracture of a S135 Drill Pipe. Procedia Materials Science, 3, 447–453. https://doi.org/10.1016/j.mspro.2014.06.075
6. Plessis, G. J., Uttecht, A., Pink, T., Hehn, L., Jellison, M. J., Vinson, B. (2016). An Innovative Pipe Grade to Enhance Reach of Deeper Prospects in Sour Fields. IADC/SPE Asia Pacific Drilling Technology Conference. https://doi.org/10.2118/180612-ms
7. Tale, S., Ahmed, R., Elgaddafi, R., Teodoriu, C. (2021). Sulfide Stress Cracking of C-110 Steel in a Sour Environment. Corrosion and Materials Degradation, 2 (3), 376–396. https://doi.org/10.3390/cmd2030020
8. Al-Mansour, M., Alfantazi, A. M., El-boujdaini, M. (2009). Sulfide stress cracking resistance of API-X100 high strength low alloy steel. Materials & Design, 30 (10), 4088–4094. https://doi.org/10.1016/j.matdes.2009.05.025
9. Vakili, M., Koutník, P., Kohout, J. (2024). Addressing Hydrogen Sulfide Corrosion in Oil and Gas Industries: A Sustainable Perspective. Sustainability, 16 (4), 1661. https://doi.org/10.3390/su16041661
10. Taravel-Condat, C., Desamais, N. (2006). Qualification of High Strength Carbon Steel Wires for Use in Specific Annulus Environment of Flexible Pipes Containing CO_2 and H2S. Volume 3: Safety and Reliability; Materials Technology; Douglas Faulkner Symposium on Reliability and Ultimate Strength of Marine Structures, 585–591. https://doi.org/10.1115/omae2006-92394
11. Ning, J., Li, H., Yoon, Y., Srinivasan, S. (2019). Review of Key Factors Related to Sour Service Material Selection for HPHT Oil & Gas Production Applications. CORROSION 2019, 1–13. https://doi.org/10.5006/c2019-13400
12. ISO 15156-1:2009(en). Petroleum and natural gas industries – Materials for use in H_2S-containing environments in oil and gas production – Part 1: General principles for selection of cracking-resistant materials.
13. Silva, C. A., Varela, L. B., Kolawole, F. O., Tschiptschin, A. P., Panossian, Z. (2020). Multiphase-flow-induced corrosion and cavitation-erosion damages of API 5L X80 and API 5DP grade S steels. Wear, 452-453, 203282. https://doi.org/10.1016/j.wear.2020.203282
14. Zheng, Y., Zhang, Y., Sun, B., Zhang, B., Zhang, S., Jin, S. et al. (2024). Corrosion Behavior and Mechanical Performance of Drill Pipe Steel in a CO2/H2S-Drilling-Fluid Environment. Processes, 12 (3), 502. https://doi.org/10.3390/pr12030502
15. Yu, Z., Zeng, D., Hu, S., Zhou, X., Lu, W., Luo, J. et al. (2022). The failure patterns and analysis process of drill pipes in oil and gas well: A case study of fracture S135 drill pipe. Engineering Failure Analysis, 138, 106171. https://doi.org/10.1016/j.engfailanal.2022.106171
16. Li, X., Lv, W., Li, M., Zhang, K., Xu, Z., Yuan, J. et al. (2024). Sulfide stress corrosion cracking in L360QS pipelines: A comprehensive failure analysis and implications for natural gas transportation safety. International Journal of Pressure Vessels and Piping, 212, 105324. https://doi.org/10.1016/j.ijpvp.2024.105324
17. Paul, S. K., Stanford, N., Hilditch, T. (2015). Effect of martensite volume fraction on low cycle fatigue behaviour of dual phase steels: Experimental and microstructural investigation. Materials Science and Engineering: A, 638, 296–304. https://doi.org/10.1016/j.msea.2015.04.059
18. Liu, M., Yang, C. D., Cao, G. H., Russell, A. M., Liu, Y. H., Dong, X. M., Zhang, Z. H. (2016). Effect of microstructure and crystallography on sulfide stress cracking in API-5CT-C110 casing steel. Materials Science and Engineering: A, 671, 244–253. https://doi.org/10.1016/j.msea.2016.06.034
19. Hazra, M., Rao, A. S., Singh, A. K. (2023). Corrosion Fatigue Failure of Exhaust Valve of a Diesel Generator. Journal of Failure Analysis and Prevention, 23 (4), 1402–1412. https://doi.org/10.1007/s11668-023-01663-2
20. Zhou, G. Y., Cao, G. H., Dong, X. M., Zhang, Z. H. (2025). Tailoring the mechanical property and sulfide stress corrosion cracking resistance of rare earth doped casing steel by tempering treatment. Corrosion Science, 245, 112699. https://doi.org/10.1016/j.corsci.2025.112699
21. Treseder, R. S., Swanson, T. M. (1968). Factors in Sulfide Corrosion Cracking of High Strength Steels. Corrosion, 24 (2), 31–37. https://doi.org/10.5006/0010-9312-24.2.31

22. Westin, E. M., Warchomicka, F. G. (2022). Solidification cracking in duplex stainless steel flux-cored arc welds Part 2 – susceptibility of 22Cr all-weld metals under high restraint. Welding in the World, 66 (12), 2425–2442. https://doi.org/10.1007/s40194-022-01389-z
23. Grobner, P. J., Sponseller, D. L., Diesburg, D. E. (1978). Effect of Molybdenum Content on the Sulfide Stress Cracking Resistance of AISI 4130-Type Steel with 0.035% Cb. CORROSION 1978, 1–21. https://doi.org/10.5006/c1978-78040
24. Liu, Y.-W., Zhang, J., Lu, X., Liu, M.-R., Wang, Z.-Y. (2020). Effect of Metal Cations on Corrosion Behavior and Surface Structure of Carbon Steel in Chloride Ion Atmosphere. Acta Metallurgica Sinica (English Letters), 33 (9), 1302–1310. https://doi.org/10.1007/s40195-020-01032-0
25. Lynch, S. (2012). Hydrogen embrittlement phenomena and mechanisms. Corrosion Reviews, 30 (3-4), 105–123. https://doi.org/10.1515/corrrev-2012-0502
26. Shi, X.-B., Yan, W., Wang, W., Zhao, L.-Y., Shan, Y.-Y., Yang, K. (2015). HIC and SSC Behavior of High-Strength Pipeline Steels. Acta Metallurgica Sinica (English Letters), 28 (7), 799–808. https://doi.org/10.1007/s40195-015-0257-1
27. Li, J., Zhou, E., Xie, F., Li, Z., Wang, F., Xu, D. (2025). Accelerated stress corrosion cracking of X80 pipeline steel under the combined effects of sulfate-reducing bacteria and hydrostatic pressure. Corrosion Science, 243, 112593. https://doi.org/10.1016/j.corsci.2024.112593
28. Chen, J., Qin, Z., Martino, T., Shoesmith, D. W. (2017). Non-uniform film growth and micro/macro-galvanic corrosion of copper in aqueous sulphide solutions containing chloride. Corrosion Science, 114, 72–78. https://doi.org/10.1016/j.corsci.2016.10.024
29. Guan, G., Wang, X., Xin, M., Sun, C., Zhang, Q., He, J. (2024). Study on the Bonding Performance of BFRP Bars with Seawater Sand Concrete. Materials, 17 (3), 543. https://doi.org/10.3390/ma17030543
30. Jiang, H., Ye, Y., Lai, S.-Y. (2023). Behavior of seawater sea sand concrete-filled plastic-lined steel tube stub columns under axial compression. Structures, 58, 105577. https://doi.org/10.1016/j.istruc.2023.105577